TABLE OF CONTENTS MAIN PAGE

CH-99-11-3

Heat and Moisture Response of Vented and Compact Cathedral Ceilings: A Test House Evaluation

Hugo Hens, Dr.Ir
Member ASHRAE

Arnold Janssens, Dr.Ir.

ABSTRACT

In the last decade, public awareness of the greenhouse effect has pushed the building sector toward higher energy efficiencies. This move has had consequences for roofs with a cathedral ceiling. A U-factor in the vicinity of 0.2 W/(m^2·K) instead of 0.6 W/(m^2·K) became the new target value. The move toward such a low U-factor for cathedral ceilings was evaluated in an extended test house program. The major objective of the research was to find answers to the following three questions: (1) What is the impact of air ingress and wind washing on the hygrothermal performance and durability of such well-insulated roofs? (2) Is a vented air space above the thermal insulation needed to prevent concealed condensation? (3) Is a vapor retarder underneath the insulation equally efficient?

The traditional answer to questions (2) and (3) is built on five assumptions: (1) heat is transported through all materials by conduction only, (2) moisture moves through the materials by diffusion only, (3) air ingress is restricted to the air space, (4) outside air ventilation functions under all circumstances, and (5) it always means additional drying capacity. The test house measurements confirmed that in the cool, maritime climate of Western Europe, air ingress and wind washing overthrow assumptions (1), (2), and (3). Also, assumptions (4) and (5) are not true under all circumstances. The research resulted in the redrafting of the performance requirements for highly insulated roofs with a cathedral ceiling.

INTRODUCTION

Until some decades ago, cathedral ceilings were an exception in domestic construction in Western Europe. As growing building costs made each cubic meter of volume valuable, the loft gradually became a living space instead of a storeroom, leading to the conversion of the traditional pitched roof into a cathedral ceiling.

Cathedral ceilings gained popularity at the moment the energy crisis stressed the need for thermal insulation. In most of those roof types, the insulation layer was installed at rafter level, above the internal lining. In the 1970s and 1980s, recommended quilt thickness did not pass 8 cm, i.e., less than half the rafter's height. As a consequence, an air space existed above the insulation. In order to counter the deleterious effects of concealed condensation, two additional rules found their way to the building site: (1) insert a vapor barrier at the inside of the thermal insulation, and (2) vent the air space above the insulation with outside air. The second rule, especially, evolved to a paradigm (Hens 1992).

As energy efficiency lost part of its impetus during the 1980s, environmental concerns took over. A widespread fear of climate change challenged governments to call for reductions in greenhouse gas emissions (IEA 1994a). One of the measures implemented was an additional decrease in U-factors for buildings, and 0.2 W/(m^2·K) became a new target at the component level. For cathedral ceilings, this means an insulation thickness up to 20 cm, i.e., the height of the rafters.

The challenges related to this higher insulation thickness were at the basis of a series of field tests on cathedral ceilings. Three questions demanded an answer:

1. What are the consequences of air ingress and wind washing for the hygrothermal performance and durability of a U ≤ 0.2 W/(m^2·K) roof?
2. Do we still need a vented air space above the thermal insulation to prevent concealed condensation?

Hugo Hens is a professor and **Arnold Janssens** is a researcher at the Laboratory for Building Physics, Department of Civil Engineering, University of Leuven, Belgium.

3. Could a vapor retarder underneath the thermal insulation be equally efficient?

Other questions, of course, also gained importance:

4. What is the durability of tiles on roofs with very low U-factors?
5. What are the optimal performance requirements for the underlay?
6. What are the risks associated with flaws in workmanship?

This paper discusses the field tests and their results. The differences between Western European and North American cathedral ceilings are clarified, and the theory and assumptions at the basis of the ventilation paradigm are presented.

DIFFERENCES BETWEEN CATHEDRAL CEILINGS IN WESTERN EUROPE AND NORTH AMERICA

In North America, cathedral ceilings are covered with a deck and finished with shingles. This results in a roof structure that is impervious to water vapor and airflow. Venting is done by coupling an air space between the insulation and the shingled deck to the outside. In Western Europe, roofs are finished with an underlay, whereon counterbattens and laths are nailed and tiles, slates, or corrugated plates are fixed (Redland 1988). In general, the roofing layers are airflow and vapor permeable. The underlay, on the contrary, which is almost always composed of overlapping 1.2 m wide strips, may be vapor permeable as well as vapor retarding. There is a further distinction between vented and compact solutions. A vented roof includes an air space between the thermal insulation and the underlay, coupled to the outside through air inlets at the gutter and outlets at the ridge. In a compact roof, the space between the underlay and the inside lining is completely filled with mineral fiber. In both cases, however, the air layer between the roofing and the underlay is wind washed, be it intentional or fortuitous.

THE CLASSIC VENTILATION THEORY

Consider a monopitch ceiling with a length of L meter (Figure 1). The distance along the pitch is y. A vented airspace separates the thermal insulation from the underlay. The thermal resistance from the inside to the upper side of the insulation (interface 1, temperature θ_1) is R_1 ($m^2 \cdot K/W$); thermal resistance from the underside of the underlay (interface 2, temperature θ_2) to the outside is R_2 ($m^2 \cdot K/W$). The related vapor resistances are Z_1 and Z_2 (both in m/s), respectively. Temperature and vapor pressure at the inside are θ_i (°C) and p_i (Pa), and sol-air temperature and vapor pressure at the outside are θ^*_e (°C) and p_e (Pa).

The average heat fluxes from inside to interface 1 ($q_{i,1}$, W/m^2) and from outside to interface 2 ($q_{e,2}$, W/m^2) conform to the following equations:

$$q_{i,1} = \frac{\theta_i - \theta_1}{R_1}; \quad q_{e,2} = \frac{\theta^*_e - \theta_2}{R_2} \qquad (1)$$

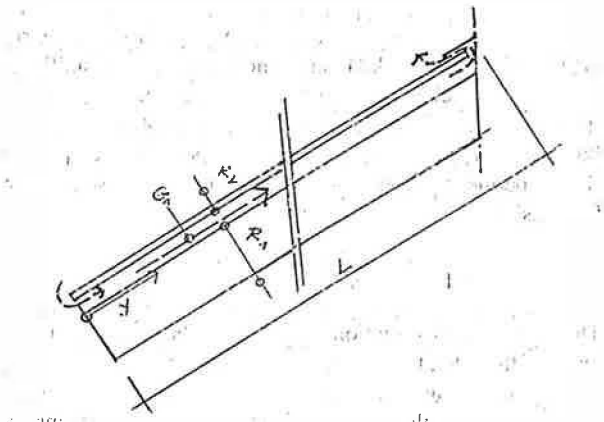

Figure 1 *Cathedral ceiling with vented air space: calculation model.*

Both equations assume heat transfer in all layers due to conduction only. In the air space, conduction splits into convection and longwave radiation. Only convection transfers heat to the venting air. This split results in the following heat balances:

$$\text{Interface 1: } \frac{\theta_i - \theta_1}{R_1} + h_{c1}(\theta_c - \theta_1) + \frac{C_b F_T(\theta_2 - \theta_1)}{1/e_1 + 1/e_2 - 1} = 0$$

$$\text{Interface 2: } \frac{\theta^*_i - \theta_2}{R_2} + h_{c2}(\theta_c - \theta_2) + \frac{C_b F_T(\theta_1 - \theta_2)}{1/e_1 + 1/e_2 - 1} = 0 \qquad (2)$$

$$\text{Cavity: } h_{c1}(\theta_1 - \theta_c) + h_{c2}(\theta_2 - \theta_c) = c_a G_a \frac{d\theta_c}{dy}$$

In the equations, C_b is 10^8 times the Stefan Bolzmann radiation constant in $W/(m^4 \cdot K)$; F_T is the temperature factor for radiation; e_1 and e_2 are the longwave emissivities of interfaces 1 and 2; h_{c1} and h_{c2} are the convection surface film coefficients at both interfaces (in $W/[m^2 \cdot K]$); c_a represents the isobaric specific heat capacity of air ($J/[kg \cdot K]$); and θ_c is the air temperature in the cavity (°C). The radiant heat transfer in the first and second equations (third term in both) is linearized. The third equation states that the air (G_a being the airflow in kg/s), while crossing the space between the insulation and the underlay from the inlet (where it starts at the outside air temperature) to the outlet, picks up convective heat. Solving the set of equations (2) for any inside temperature, any outside sol-air temperature, and any airflow gives the temperatures in the air space and the temperatures at both interfaces 1 and 2.

The airflow G_a, in turn, is wind pressure and stack driven. Its magnitude depends on the permeance coefficient a_c of the air space (in $kg/[s \cdot Pa^{0.5}]$):

$$G_a = a_c \left[\Delta P_a + \frac{g P_a}{R_a T_m^2} L \sin(h)(T_c - T_e) \right]^{0.5} \qquad (3)$$

Between brackets is the sum of the wind pressure difference and the stack effect. In the stack part, h represents the slope of the roof, T_c the harmonic mean of the cavity temper-

ature, and T_e the outside temperature, both in K. The term $gP_a/R_aT_m^2$ reduces to 0.043 under normal ambient conditions. In it, g is the acceleration by gravity in m/s^2, P_a the mean atmospheric pressure in Pa, R_a the gas constant of air in Pa·m^3/(kg·K), and T_m the mean temperature along the stack path in K. The permeance coefficient a_c is defined by the sum of the flow resistance in the air space:

$$a_c = [0.625/A_{in}^2 + 0.625/A_{out}^2 + W_c]^{-0.5} \quad (4)$$

The first term in Equation 4 represents the hydraulic resistance of the inlet, the second term the hydraulic resistance of the outlet, and the third term the hydraulic resistance of the cavity. A_{in} is the inlet and A_{out} the outlet area in m^2 per running meter monopitch.

If diffusion is assumed to be the only vapor transfer mechanism through all material layers between the air space and the inside and outside environment, then the vapor balance of the air space is as follows (ρ_a being the density of air in kg/m^3, R_v the gas constant for water vapor in Pa·m^3/[kg·K], and T the temperature in K):

$$\frac{p_1 - p_c}{Z_1} + \frac{p_2 - p_c}{Z_2} = \frac{G_a}{\rho_a R_v T}\frac{dp_c}{dy} \approx 6.21 \times 10^{-6} G_a \frac{dp_c}{dy} \quad (5)$$

with, as a solution,

$$p_c = p_{c\infty} + (p_e - p_{c\infty}) \exp\left(\frac{1}{6.21 \times 10^{-6}} \frac{(Z_1 + Z_2)y}{Z_1 Z_2 G_a}\right) \quad (6)$$

where

$$p_{c\infty} = \frac{Z_1 p_e + Z_2 p_i}{Z_1 + Z_2} \quad (7)$$

The value $p_{c\infty}$ represents the vapor pressure in the nonvented air space. In the cold season, concealed condensation starts when, at $y = L$, p_c equals the vapor saturation pressure p_{sat1} on interface 1 or the vapor saturation pressure p_{sat} belonging to the lowest interface temperature between the air space and the farthest exterior layer. Both values hardly differ from the outside vapor saturation pressure. As a consequence, a safe upper threshold for the ventilation flow to avoid concealed condensation conforms with the following equation:

$$G_{a,min} = \frac{161000(Z_1 + Z_2)L}{Z_1 Z_2 \ln\left(\frac{P_{sat,e} - P_{c\infty}}{p_e - p_{c\infty}}\right)} \quad (8)$$

Implementing $G_{a,min}$ in Equation 3 gives the minimum inlet and outlet area in m^2 per running meter roof. In the classic approach, Equations 8 and 3 are solved for a cold, cloudy day with a probability of occurrence once a year. Only the stack effect is considered as active force, while the vapor resistance of the exterior layer Z_2 is fixed at a high value. Independent of any calculation, Equations 7 and 8 inspired some straightforward conclusions:

- A ventilation flow higher than $G_{a,min}$ should function under all (less negative than assumed) circumstances.
- Adding a vapor retarder at the inside diminishes the need for ventilation. In fact, a vapor retarder brings $p_{c\infty}$ close to p_e and G_a down to zero.
- Combining ventilation with a vapor retarder should reduce the risk of concealed condensation to an absolute minimum, a decision that may figure as an example of a redundant protective measure (Bomberg and Lstiburek 1998).

Criticism of Classic Ventilation Theory

By far the weakest point in the classic ventilation theory is the assumption that both the inside and outside part of a vented cathedral ceiling are perfectly airtight. Experiences and measurements in practice prove the opposite. Latta (1974) already mentions air intrusion as a major cause of concealed condensation. Orr (1974) reports on attic condensation problems in electrically heated houses, the main reason being air leakage from inside. Rousseau (1984) stresses that air leakage can transport 100 times as much water vapor as diffusion does. Recently, IEA Annex 19 (IEA 1994b) noted this reality in its guidebook on insulated low-slope roof systems. Künzel (1997) describes an on-site research program that confirms airflow to be a major contributor to moisture degradation in sloped roofs. ASHRAE (1997) in its *1997 Fundamentals* also quotes air movement as one of the main moisture transport mechanisms. Even cathedral ceilings with a vapor retarder happen to be very air permeable, as was experienced during damage case investigations (LBP 1981, 1994). Air ingress changes the hygrothermal response completely. Heat and vapor transfer become convection driven. As mentioned by Rousseau, the risk of concealed condensation increases dramatically.

By using a cold cloudy day as the reference, longwave radiation is overlooked in the theory. This phenomenon may turn the outside air into a moisture source instead of a drying medium. Also, the assumption of a monopitch is primitive with regard to the way airflow develops in real roofs within the air space between the thermal insulation and the underlay. Some of the simplifications are even too pessimistic. The hypothesis, for example, that the exterior part is vapor tight should not be true (Janssens and Hens 1997). Also hygroscopic buffering is not taken into account, as is moisture release by self-drainage.

FIELD TESTING

The field tests were started in 1986. A monopitch test building with a sloped surface of 334 cm × 622 cm, 35° from horizontal, facing northeast, was constructed on top of the flat roof covering a laboratory and divided into four fields of 163.4 cm, 147.6 cm, 147.6 cm, and 163.4 cm each, as shown in Figure 2 [(Hens et al. 1992; Hens 1994).

BACK TO PAGE ONE

The four fields, with a monopitch length of 334 cm, contained different cathedral ceiling sections. In total, five series of four sections each were tested (see Table 1 for details). All sections had thermocouples and heat transducers at 47 cm, 167 cm, and 287 cm from the gutter along the pitch. Detachable parts were included in the underlay and the insulation so as to match the moisture accumulation at regular time intervals. Some sections got air pressure taps. The test building was heated with four IR bulbs of 250 W each, coupled to a proportional temperature controller. Free evaporation from a water surface of 1.2 m^2 humidified the air. Indoor temperature and relative humidity were logged in the center of the building enclosure 1.5 m above floor level. Monitoring of the outdoor climate included temperature, relative humidity, and precipitation.

Figure 2 *Test building for the monopitch cathedral ceilings.*

TABLE 1
Monopitch Sections from Outside to Inside
(FCC = Fiber Cement, MF = Mineral Fiber)

Section Series	1	2	3	4
1.	· Tiles · Laths and Battens · FCC as Underlay · 20 cm MF · Polyethylene Film · Cavity, 22 mm · Gypsum Board	· Tiles · Laths and Battens · FCC as Underlay · Vented Air Space · 8 cm MF · Paper Facing · Gypsum Board	No part of the vented-compact comparison	No part of the vented-compact comparison
2.	Same as series 1, lath ceiling instead of gypsum board			
3.	Same as series 2, the capillary FCC underlay replaced by a noncapillary, perforated, glass-fiber-reinforced foil with a band width of 1.2 m and an overlap of 0.1 m			
4.	· Tiles · Laths and Battens · Foil as Underlay · 20 cm MF · Polyethylene Film · Cavity, 22 mm · Lath Ceiling	· Tiles · Laths and Battens · Foil as Underlay · 20 cm MF · Lath Ceiling	· Tiles · Laths and Battens · Foil as Underlay · 20 cm MF · Gypsum Board	· Tiles · Laths and Battens · Foil as Underlay · 12 cm MF
5.	· Tiles · Laths and Battens · CFF as Underlay · 20 cm MF · Polyethylene Film · Cavity, 22 mm · Gypsum Board	· Tiles · Laths and Battens · CFF as Underlay · 20 cm MF · Gypsum Board	· Slates · Laths and Battens · CFF as Underlay · 20 cm MF · Polyethylene Film · Cavity, 22 mm · Gypsum Board	· Slates · Laths and Battens · CFF as Underlay · 20 cm MF · Gypsum Board

BACK TO PAGE ONE

A first series of four roofs was tested from December 1986 to October 1987, when the inside gypsum board lining was exchanged for an air-permeable lath ceiling. The second series started on November 1987 and lasted until November 1988, when the capillary, vapor-permeable fiber, cement underlay (FCC) was replaced by a vapor-retarding, noncapillary foil. Monitoring of this third series started in January 1989 and stopped in November 1989. At that moment, all roofs except section 1 were refurbished. Series four started in January 1990 and lasted until May 1991. After a final reconstruction of all sections, the fifth and last series was monitored from December 1991 until June 1993.

In 1995, a new test building, called the VLIET building (see Figure 3), was constructed in an open field, close to the Dyle River, near Leuven (Janssens and Hens 1995). This building allows the monitoring of six duopitch cathedral ceilings, with a span of 720 cm each, a width of 1.8 m, and a slope of 45°. For details of the sections, see Table 2. All had thermocouples, heat transducers, air pressure tabs, condensation sensors, and moisture pins inserted at three heights to log temperatures, heat fluxes, periods of condensation, and moisture content in the rafters. Inside the building, air temperature, vapor pressure, and air pressure were controlled. The outdoor climate is monitored in full detail close to the building, including temperature, relative humidity, precipitation, wind velocity and direction, and solar gains. Monitoring of the test sections started in December 1996.

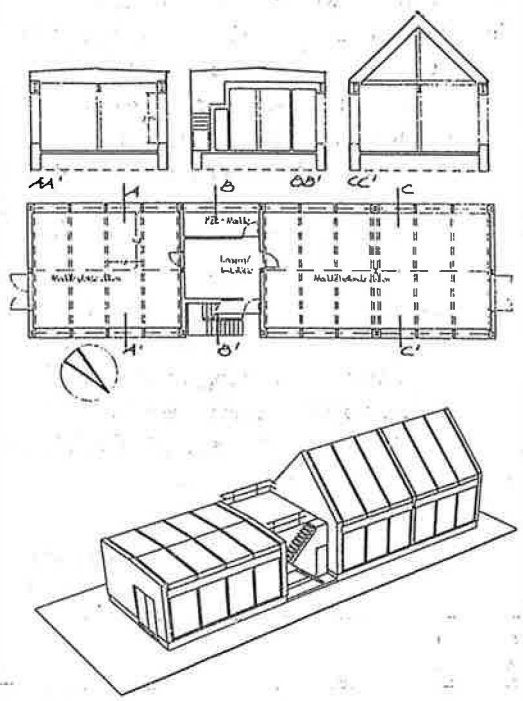

Figure 3 VLIET test building.

TABLE 2
Duopitch Sections from Outside to Inside
(MF = Mineral Fiber)

1	2	3
· Tiles · Laths and Battens · Vapor-Permeable Foil as Underlay · 20 cm MF · Polyethylene Film · Cavity, 50 mm, Filled with MF · Gypsum Board, Finished with Acrylic Paint	· Tiles · Laths and Battens · Vapor-Permeable Foil as Underlay · 20 cm MF · Cavity, 50 mm, Filled with MF · Gypsum Board, Finished with Acrylic Paint	· Tiles · Laths and Battens · Bituminous Underlay · Vented Air Space, 5 cm · 15 cm MF · Polyethylene Film · Cavity, 50 mm, Filled with MF · Gypsum Board, Finished with Acrylic Paint
4	**5**	**6**
· Tiles · Laths and Battens · Bituminous Underlay · Vented Air Space, 5 cm · 15 cm MF · Cavity, 50 mm, Filled with MF · Gypsum Board, Finished with Acrylic Paint	No Part of the Vented-Compact Comparison	No Part of the Vented-Compact Comparison

RESULTS

Test Series 1, 2, and 3, Monopitch Cathedral Ceilings

Series 1,2, and 3 had as their main objective comparison of the hygrothermal response of a compact cathedral ceiling with airflow and vapor retarder on the inside, called section 1, with a vented cathedral ceiling, called section 2. Section 1 had a clear wall U-factor of 0.15 W/(m^2·K) and was composed as follows (from inside to outside): gypsum board internal lining (exchanged before series 2 started for a lath ceiling), air space of 2.6 cm, 0.2 mm thick polyethylene foil as airflow and vapor retarder, 20 cm of medium-weight mineral fiber (called MF in Table 1), 3.2 mm thick fiber cement underlay (called FCC in Table 1 and exchanged before series 3 started for a plastic foil underlay), counterbattens, laths, and tiles. Section 2, with a clear wall U-factor of 0.4 W/(m^2·K), included (from inside to outside): gypsum board internal lining (exchanged before series 2 started for a lath ceiling), 8 cm of medium-weight mineral fiber with paper facing, 12 cm high vented air space, 3.2 mm thick fiber cement underlay (exchanged before series 3 started for a plastic foil underlay), counterbattens, laths, and tiles. The successive three test series allowed evaluation of (1) the difference in behavior between a vapor-permeable, capillary FCC underlay, which should minimize concealed condensation, and a vapor-retarding, noncapillary plastic foil underlay (series 1 vs. series 2), and (2) the effect of an airtight, vapor-permeable inside lining—gypsum board—in comparison with a less vapor-permeable but more airflow-permeable inside lining, a lath ceiling (series 1 and 2 vs. series 3). Workmanship in the compact section 1 was optimal. Instead, the vented section 2 was an exemplary case of normal workmanship, with all flaws typical for daily building practice: paper facing of the insulation not overlapping at the rafters, quilts not covering the whole surface, etc.

Climate. Figure 4 gives the monthly average indoor and outdoor temperatures and vapor pressures and total precipitation outside. The outside climate is cool, humid, and wet. The difference in inside-outside vapor pressure (Pa) totaled:

Series 1: $\Delta p_{ie} = 348 \quad 9.9\ \theta_e$

Series 2: $\Delta p_{ie} = 469 - 12.5\ \theta_e$

Series 3: $\Delta p_{ie} = 824 - 39.4\ \theta_e$

This shows that during series 1 and 2 the inside climate could be quoted as rather dry, while during series 3 it was more humid. These differences should be compared with the average and 90% percentile, measured in a total of 20 inhabited loft spaces (vapor pressure difference in Pa):

Average: $\Delta p_{ie} = -134 - 49.4\ \theta_e + 51.2\ \theta_i$

90% percentile: $\Delta p_{ie} = 108 - 49.4\ \theta_e + 51.2\ \theta_i$

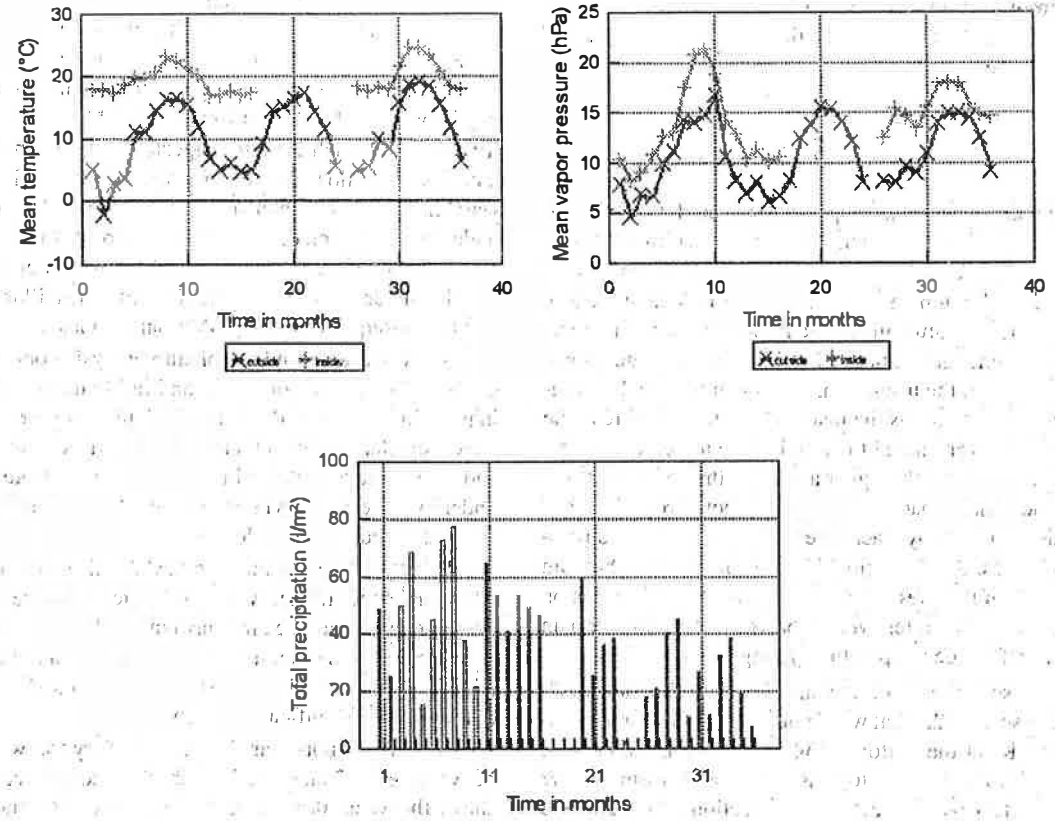

Figure 4 Indoor and outdoor climate during series 1, 2, and 3.

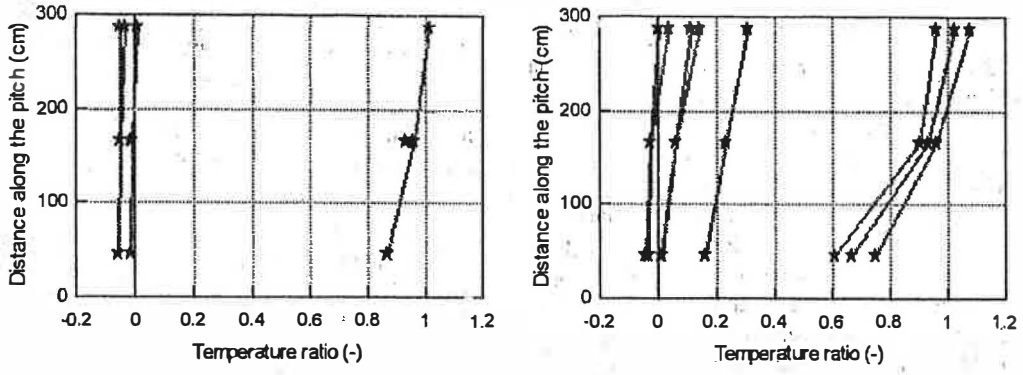

Section 1 *Section 2*

Figure 5 *Average winter temperature ratios in the two sections during series 1. The highest values represent the inside surface, the lowest to the outside surface. Lines in between relate to the following interfaces: for section 1 (from lowest to highest), underside of the tiles and topside of the underlay, topside of the internal lining; for section 2 (from lowest to highest), underside of the tiles, topside of the underlay, underside of the underlay, topside of the insulation, underside of the insulation, topside of the internal lining, underside of the internal lining.*

For 18°C inside, the average and the 90% percentile become 787 – 49.4 θ_e and 1029 – 49.4 θ_e, respectively, underlining that the values for the test house are realistic.

Thermal Response. Figure 5 shows the average winter temperature ratios measured in sections 1 and 2. Temperature ratios are defined as:

$$f_y = \frac{\theta_y - \theta_e}{\theta_i - \theta_e} \tag{9}$$

with θ_y the temperature in the point considered, θ_i the inside and θ_e the outside reference temperature. f_y is a dimensionless temperature. While the results for section 1 (with a somewhat lower inside lining temperature at the bottom than at the top, a mid-height temperature in between, and an underlay temperature a little higher at the top than at the bottom) suggest some air rotation around the insulation, rotation in section 2 is obviously present. Not only is the inside lining temperature at the bottom much lower than at the top, but the underlay temperature is also significantly higher at the top than at the bottom. Air from the vented space and outside air both protrude under the insulation, partly by stack effect and partly by wind pressure differences. Also, section 1, as section 2, suffers from undercooling of the tiles. The temperature ratio measured on top of the tiles on a winter average basis is, in fact, lower than the outside reference temperature (f_y negative).

The consequences for the insulation quality are quite negative. In section 2, local winter heat loss inside amounts to 0.87 W/(m^2·K) at the bottom, 0.34 W/(m^2·K) in the middle, and 0.56 W/(m^2·K) at the top instead of a uniform 0.4 W/(m^2·K), the clear wall U-factor of the section. On average, a loss of 0.6 W/(m^2·K) is noted, 50% higher than the 0.4 W/(m^2·K) expected. At the underlay, the apparent thermal performance looks better, with an average of 0.37 W/(m^2·K), i.e., lower than the clear wall value. These differences in average U-factor between the underlay and inside confirm that exterior air protrudes under the insulation layer.

In series 2, with the airflow-retarding gypsum board replaced by an air-permeable lath ceiling, heat loss changes. An average of 0.43 W/(m^2·K) is noted at the inside lining in section 2. The underlay now gives 0.4 W/(m^2·K). The main cause for that difference with series 1 is additional air intrusion from inside, which is also suggested by the winter average temperature ratios (see Figure 6). The inside lining stays warmer in series 2 than in series 1. Simultaneously, more undercooling is noted, an explanation for this being the drier series 2 winter. The switch in series 3 from a vapor-permeable, capillary underlay to a vapor-retarding, noncapillary underlay had no consequences for the thermal response.

Moisture Response. Moisture analysis concentrated on concealed condensation under and in the underlay, moisture ingress in the counterbattens and laths, and wetting of the water-repellant and non-water-repellant tiles. During series 1 and 2, moisture content in the vapor-permeable, capillary underlay increased in winter and decreased in summer for both sections 1 and 2 (see Table 3).

In none of the sections, however, did accumulation pass the hygroscopic range, while the values measured showed a net correlation with the underlay temperature—the higher this was, the lower the maximum moisture content was. Ventilation of the air space between the insulation and the underlay did not have a significant influence.

After the vapor-retarding, noncapillary foil was installed between series 2 and 3, things changed completely. Figure 7 shows the weeks during the one year of testing when droplets were noted under the foil. While the underlay of section 1 suffered from droplets the first winter only, as a consequence of the condensation of moisture that entered the roof during

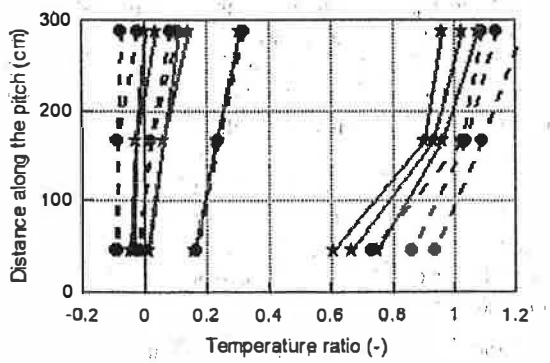

Figure 6 *Average winter temperature ratios in section 2 during test series 1 and 2, a comparison. The dots represent series 2, the stars series 1. The highest values represent the inside surface, the lowest to the outside surface. Lines in between relate from lowest to highest to the following interfaces: underside of the tiles, topside of the underlay, underside of the underlay, topside of the insulation, underside of the insulation, topside of the internal lining, underside of the internal lining.*

TABLE 3
Moisture Content and Relative Humidity in the Vapor-Permeable, Capillary Fiber, Cement Underlay During Test Series 1 and 2
(Capillary Moisture Content: 320 kg/m^3)

Series	Section 1		Section 2	
	Winter	Summer	Winter	Summer
1. w	161 kg/m^3	132 kg/m^3	139 kg/m^3	100 kg/m^3
RV	98%	94%	95%	89%
Temp.	−0.015		0.06	
2. w	195 kg/m^3	150 kg/m^3	141 kg/m^3	101 kg/m^3
RV	>99%	96%	95%	89%
Temp.				

underlay refurbishment, section 2 shows abundant droplet formation during the second as well as the first winter. Venting the air space above the insulation clearly does not prevent concealed condensation from occurring. This was also illustrated by the weight changes between summer and winter in the loose parts in the underlay (see Table 4). The restricted moisture deposit in section 1 is mainly caused by migration, during the winter, of hygroscopic moisture from the rafters up to the underlay. In section 2, instead, where winter deposit is much higher, the minimum at the top confirms the existence of buoyancy-induced air rotation around the thermal insulation, resulting in a stream of warm air that hit the underlay there.

TABLE 4
Maximal Moisture Deposit Against the Underlay in Winter During Test Series 3 (n·kg/m^2)

Section 1			Section 2		
Bottom	Middle	Top	Bottom	Middle	Top
0.380	0.320	0.330	0.615	0.672	0.353

The wet winter during test series 1 humidified the timber laths intensively. Moisture ratios, measured with electrical resistance pins, gave 80% by weight at several intervals. The problem was less pronounced during the drier winters of test series 2 and 3, when moisture ratios went down to values just above 20% by weight. Moisture above 20% may induce severe fungal attack in the laths.

During all three test series, the non-water-repellent tiles underwent a winter/summer moisture transient. They turned wet in autumn, stood wet the whole winter at a moisture content close to capillary, and dried in the spring, In summer, they changed from dry to wet according to the rhythms of the rainfall. The water-repellent tiles instead picked up some moisture in autumn and winter but dried in summer. Undercooling was responsible for the wet winter situation. As noticed above, undercooling keeps the winter average tile temperatures not only below the outside air temperature but also below the outside dew-point temperature.

Durability. During series 1, 2, and 3, the durability analysis focused on the temperature extremes in the tiles and the

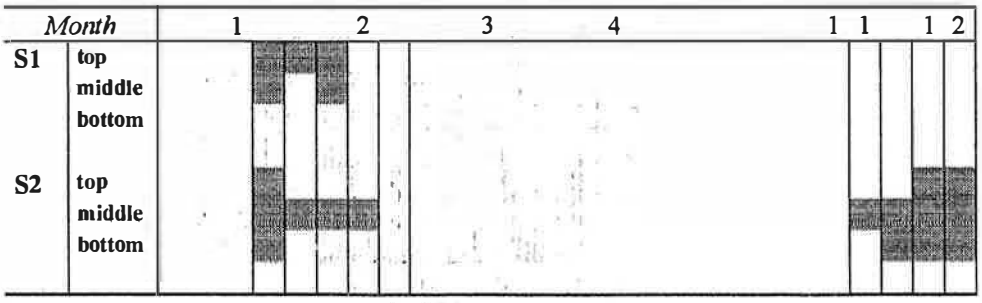

Figure 7 *Condensation droplets underneath the underlay foil during series 2. Gray represents the weeks when droplets were noted.*

frost/thaw cycles they underwent. The highest tile temperature noted in summer for section 1 was 57.4°C and 52.6°C for section 2. Undercooling extremes were 5.9°C below air temperature for section 1 and 5.7°C below for section 2. The number of frost/thaw cycles is summarized in Table 5. Apparently, the number of cycles in the tiles is higher than in the air. However, as far as both durability aspects are concerned, the two sections behave in a similar manner.

TABLE 5
Number of Frost/Thaw Cycles in Sections 1 and 2 in Relation to the Number of Days with a Temperature Below Zero During Test Series 1, 2, and 3

Series	Number of Days	Section 1	Section 2
1	37	62	69
2	3	9	8
3	11	16	15

Series 4 and 5, Monopitch Cathedral Ceilings

Series 1, 2, and 3 showed that vented cathedral ceilings, constructed according to "normal" workmanship, bring no benefit for the hygrothermal response in humid, cool climates. Therefore, the vented section was abandoned in series 4. Section 2 and section 3, which were not part of the compact vs. vented investigations during test series 1, 2, and 3, were refurbished as compact roofs with the same insulation thickness as section 1. Neither section 2 nor section 3, however, got an airflow- and vapor-retarding polyethylene film underneath the insulation. Instead, section 2 was finished with an air-permeable groove and tongue lath ceiling and section 3 with an airflow-retarding, vapor-permeable gypsum board. In both cases, workmanship was very good. Section 4, which was also used for other purposes during test series 1, 2, and 3, figured as an extreme case now, with no internal lining, no airflow and vapor retarder, and poor workmanship. Series 1, 2, and 3 had a clear wall U-factor of 0.15 W/(m^2·K), and series 4 had a clear wall U-factor of 0.22 W/(m^2·K). Workmanship in section 1 remained optimal.

Series 5 continued testing of compact ceilings. All sections were completely refurbished. In section 1 and 2, glazed ceramic tiles replaced the existing ones. Section 1 also got a vapor-permeable, capillary fiber cement underlay, 20 cm of fiberglass, an airflow- and vapor-retarding polyethylene foil, a small cavity on the inside, and a gypsum board internal lining. Section 2 was identical, except for the airflow and vapor retarder. The only difference between sections 3 and 1 was the roofing—slates instead of tiles. Section 4 was a copy of section 3 without the airflow and vapor retarder. Workmanship in the four sections was less perfect than it was in the compact section 1 of series 1, 2, 3, and 4. At the top, a leak was left in the polyethylene foil and the gypsum board. In the foil, the incision was retaped as well as possible before mounting the inside lining. The leaks in the internal lining, on the other hand, remained uncaulked.

Climate. Figure 8 shows the monthly average inside and outdoor temperatures and vapor pressures plus the precipita-

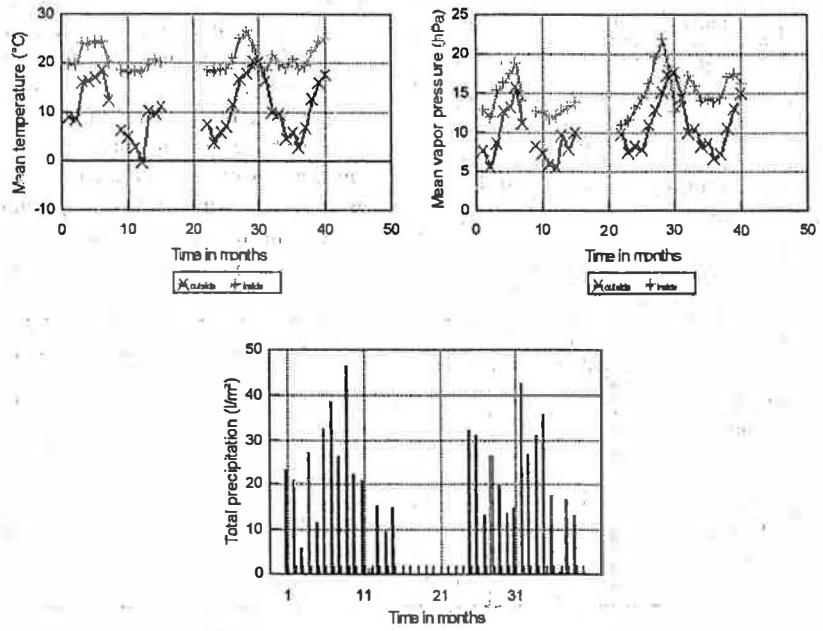

Figure 8 Indoor and outdoor climate during series 4 and 5.

tion outside. The difference in inside-outside vapor pressure was:

Series 4: $\Delta p_{ie} = 724 - 28.4\ \theta_e$

Series 5: $\Delta p_{ie} = 524 + 5.16\ \theta_e$

During both series, the inside climate was rather wet, although still in line with the values measured in inhabited loft spaces.

Thermal Response. During series 4, the average winter temperature ratios in section 1 were comparable to those measured in series 1, 2, and 3. Figure 9 gives the average winter temperature ratios in sections 2 and 3. In section 2, temperature ratios shift to higher values than in section 3. This underlines that buoyancy-induced flow around the thermal insulation is only one of the mechanisms that deteriorate thermal performance. Section 2, with its air-permeable lath ceiling, also suffers from air intrusion from inside more than section 3 does with its airtight gypsum board ceiling. Section 4 showed extreme behavior, with a very active air exfiltration at the top and infiltration at the bottom of the pitch.

During series 5, the impact of the leaks on the temperature profile was quite pronounced for the sections without polyethylene foil, as illustrated by Figure 10. Again, some buoyancy flow around the insulation develops. In section 2, however, air intrusion from inside through the leak dominates. The winter average heat fluxes underline that reality. In sections 1 and 3, both with some leakage in the airflow and vapor retarder, a small difference exists between the fluxes at the inside lining and those along the underlay (see Table 6). Hence, even those small differences suggest the insulation in both sections to be wind washed from top to bottom. In sections 2 and 4, however, the flux is significantly higher at the underlay than at the inside lining. Moreover, in section 2, the one with the tiles, the underlay flux peaks at the top of the pitch.

Air Intrusion. A separate study mapped the air transport in the four sections during series 5. For that purpose, a two-day CF_6 tracer test was conducted. The first four hours, the tracer was injected in the test building at a constant rate and the concentrations in the building and all four sections were logged. Tracer concentration increased rapidly in sections 2 and 4, both constructed without airflow retarder, to reach a constant value that was hardly different from the concentration in the test building. In sections 1 and 3, instead, concentration buildup progressed slowly at the bottom, while at the top an equilibrium was reached quickly, albeit at a concentration below the one in

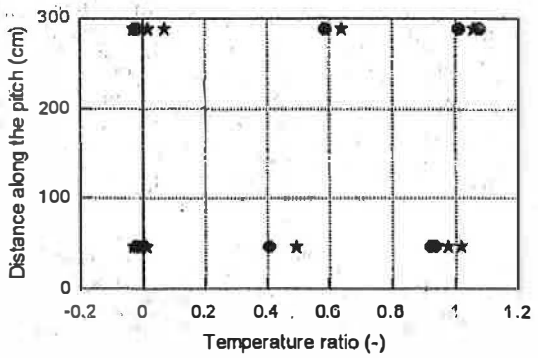

Figure 9 *Temperature ratios in sections 2 (stars) and 3 (dots) during series 4. The highest values represent the inside surface, the lowest to the outside surface. Lines in between relate from lowest to highest to the following interfaces: underside of the tiles and topside of the underlay, topside of the internal lining. The in between values are taken at half the thickness of the thermal insulation.*

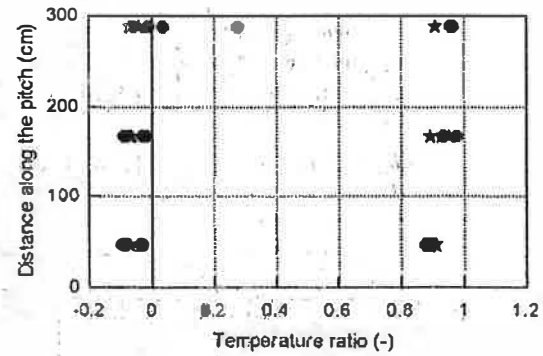

Figure 10 *Temperature ratios in sections 1 (stars) and 2 (dots) during series 5. The highest values represent the inside surface, the lowest to the outside surface. Lines in between relate from lowest to highest to the following interfaces: underside of the tiles and topside of the underlay, topside of the internal lining.*

TABLE 6

Winter Average Heat Fluxes in Sections 1, 2, 3, and 4 During Test Series 5 (W/m²)

Series 5	Section 1			Section 2			Section 3			Section 4		
	Bottom	Middle	Top	Bottom	Middle	Top	Bottom	Middle	Top	Bottom	Middle	Top
Underlay	2.3		1.5	3.0		4.1	2.0		2.3	2.6		2.7
Inside	1.8		2.0			2.0	2.5		2.5			2.0

the test building. The results showed that ventilation in the test building reached 5.2 h^{-1}, a flow of 84 m^3 /h. Of this 84 m^3/h, 2.4 m^3/h was exfiltrated through sections 2 and 4. Simultaneous wind washing in both sections was responsible for an airflow between the underlay and inside lining of some 0.5 m^3/h. At the leak in section 3, outside air washing was two times as important as the exfiltration flow. In section 1, instead, the ratio between exfiltration and outside air washing scattered around 4 to 1.

During the second four hours, tracer was injected at the bottom of section 2, under the insulation. Matching the tracer along the pitch revealed a slow concentration increase in the middle and at the top. Concentration just under the underlay, however, remained very low. Apparently, infiltration and exfiltration act simultaneously with wind washing. The next day, the tracer was injected directly under the tiles and slates and logged along the pitch at both sides of the underlay. Two conclusions could be drawn from the results. First, ventilation under the tiled and slated deck is a fact, even when no specific venting features are present. Second, wind washing brings tracer into the section, even as far as below the thermal insulation.

Moisture Response. Moisture analysis included concealed condensation underneath and in the underlay and

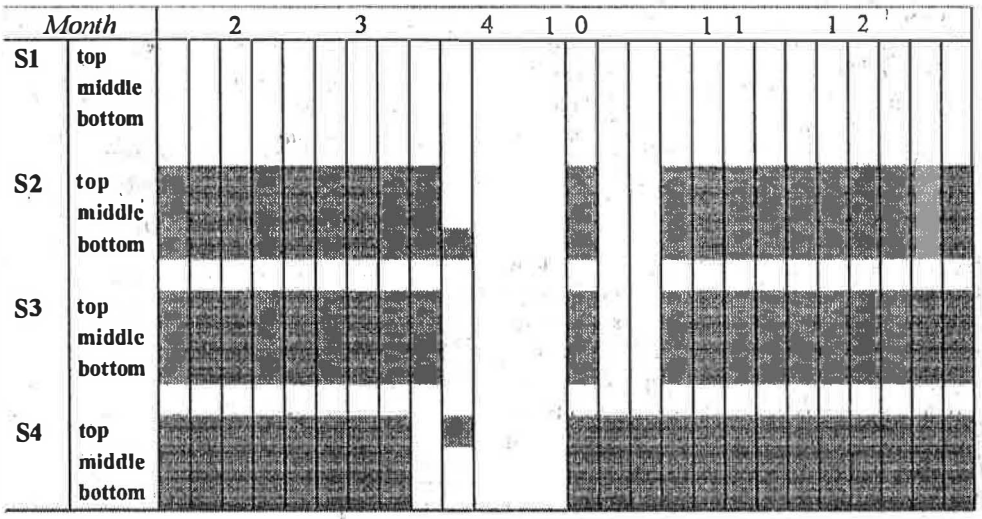

Figure 11 *Condensation droplets underneath the underlay foil during series 4. Gray represents the weeks when droplets were noted.*

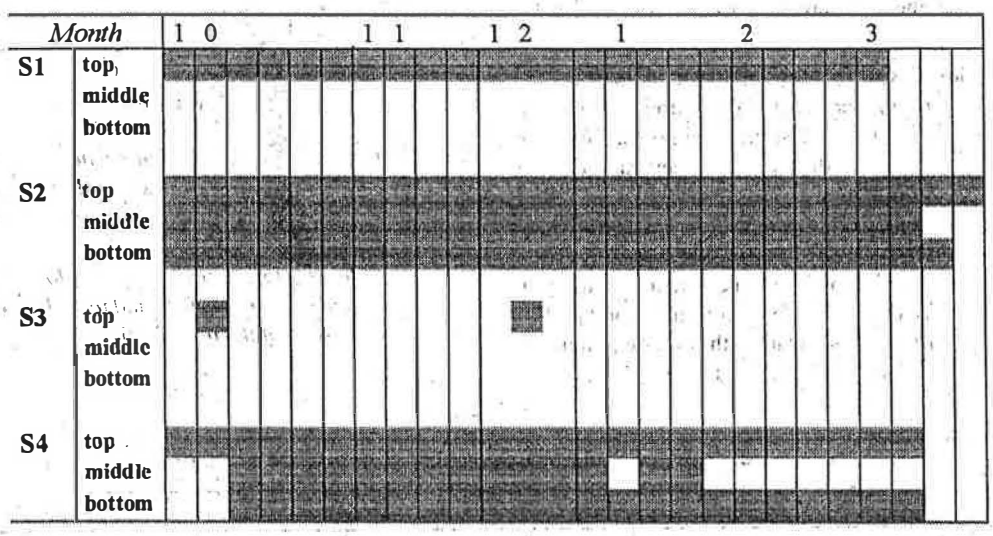

Figure 12 *Condensation droplets underneath the FCC underlay foil during series 5. Gray represents the weeks when droplets were noted.*

BACK TO PAGE ONE

TABLE 7
Maximal Moisture Deposit Under and In the Underlay at the End of the Winter During Test Series 4 and 5 (kg/m²)

Series	Section 1 Reference			Section 2 No PE Film Lath Ceiling			Section 3 No PE Film Gypsum Board			Section 4 No Inside Lining		
	Bottom	Middle	Top	Bottom	Middle	Top	Bottom	Middle	Top	Bottom	Middle	Top
4, Foil	0.82	0.94	1.12	5.03	4.10	4.94	4.66	3.41	4.24	3.96	6.65	8.65
Insulation											1.00	
Series	**Section 1 PE Film**			**Section 2 No PE Film**			**Section 3 PE Film**			**Section 4 No PE Film**		
	Bottom	Middle	Top	Bottom	Middle	Top	Bottom	Middle	Top	Bottom	Middle	Top
5, FCC	0.34	0.32	0.80	0.59	0.80	1.40	0.33	0.43	0.55	0.58	0.54	0.92
Insulation	0	0	0.39	1.9	1.0	0.86	0	0.21	0.27	0.84	0.49	0.81

wetting of rafters, laths, and tiles. Figures 11 and 12 show the successive winter weeks within test series 4 and 5 during which droplets were noted underneath the underlay (foil and FCC). Table 7 summarizes moisture deposit in the underlay and the insulation at the end of each winter. Deleting the airflow and vapor retarder, as was done in sections 2, 3, and 4 of series 4 and sections 2 and 4 of series 5, is a negative decision. Abundant condensation is the consequence. The quantities measured during series 4, however, do not correlate with the vapor permeance of the inside lining, which is six times lower for the lath ceiling of section 2 than for the gypsum ceiling of section 3 ($K_p = 2.15\times10^{-10}$ s/m vs. $K_v = 1.3\times10^{-9}$ s/m). Most moisture condenses in section 2. Apparently, the higher air permeance of the lath ceiling ($K_a = 4.1\times10^{-4}\ \Delta P_a^{-0.37}$ s/m vs. $3.1\times10^{-5}\ \Delta P_a^{-0.2}$ s/m for the gypsum board) causes more concealed condensation. On the other hand, flaws in workmanship, such as leaks, substantially diminish retarder efficiency. Compare for that purpose section 1, series 4, with sections 1 and 3, series 5. The difference in moisture response is striking—neither droplets nor moisture deposits in section 1, series 4, and not only droplets but also more moisture deposit near the leaks in sections 1 and 3, series 5. Also, a vapor-permeable, capillary underlay does not exclude droplet formation in roofs without airflow and vapor retarder and leaks in the inside lining, as shown by sections 2 and 4, series 5.

During both test series, laths picked up moisture to a level that could induce serious fungal attack. Moisture content in the tiles reflected the same periodicity as seen during series 1, 2, and 3. The water-repellent tiles, however, slowly lost part of their repellency. Glazed tiles, instead, dried only partially during summer, and slates got wet by undercooling, rather than by precipitation.

Durability. The highest summer temperatures, undercooling effects, and frost/thaw cycles noted in the tiles, the slates, and the air were in line with the results of series 1, 2, and 3.

Series 6, Duopitch Cathedral Ceilings

Monopitch ceilings are not as common as duopitch ceilings, which is why they were tested in the new test building. At the present time, six sections with $U<0.2$ W/(m·K) are under scrutiny: two vented, two compact, one prefab, and one retrofit. One of the two vented sections and one of the two compact sections has an airflow and vapor retarder underneath the thermal insulation, and the other two do not. In both compact sections, a vapor-permeable underlay is used. The vented sections have instead a vapor-retarding underlay.

After one year of testing, most of the conclusions for monopitch ceilings were confirmed. Wind washing and air intrusion are the major problems. Wind washing makes the thermal resistance wind-dependent. Venting the air space between the insulation and the vapor-retarding underlay does not turn the hygrothermal performance from problematic to correct. On the contrary, the two vented sections suffer more from undercooling-related condensation than the compact sections do. SF_6 tracer testing showed that when wind-driven ventilation prevails, the largest part of the ventilation flow passes from the southwest to the northeast pitch. Only when stack flow overcomes wind-driven ventilation, air is sucked in at the eaves and released at the ridge. This short circuit between the two pitches allows the ventilation air to pick up moisture at the warmer southwest side and deposit it at the cooler northeast side.

CONCLUSIONS

This research started with three questions: (1) What are the consequences of air ingress and wind washing for the hygrothermal performance and durability of highly insulated cathedral ceilings? (2) Do we still need a vented air space above the thermal insulation to prevent concealed condensation? (3) Could a vapor retarder underneath the insulation be equally efficient?

Test series 1, 2, and 3 on monopitch ceilings gave part of the answer for humid, cool climates. The airflow and vapor-

retarding, highly insulated compact section 1, with good workmanship as one of its characteristics, showed satisfactory hygrothermal behavior—there was only a marginal presence of buoyancy flow around the insulation and no harmful concealed condensation. The vented section 2, with workmanship in accordance with normal practice, did not behave in an acceptable way—there was important buoyancy flow around the insulation, intrusion of outside air underneath the insulation, a significant increase in the equivalent U-factor, and unacceptable concealed condensation when a vapor-retarding, noncapillary underlay was used. Test series 4 and 5 completed that picture. A compact section functions in a correct way only when airtightness is guaranteed. Different modes of airflow must be considered, not only infiltration and exfiltration but also wind washing and buoyancy-induced air rotation around and in the insulation. These airflow modes act simultaneously. In search for solutions, installing an airflow and vapor retarder at the inside does not suffice. An underlay open to wind and insulation mounted in such a way that air rotation is favored should also be avoided. Furthermore, lack of airtightness is not fully compensated by a vapor-permeable, capillary underlay. Although performance is better than with a vapor-retarding foil, concealed condensation with droplet formation remains a problem. Also, compact roofs demand good workmanship. Flaws, such as air leaks in the retarder, may influence the overall hygrothermal response in a very negative way. Finally, airtightness is not all that is required. Correct vapor resistance is also needed.

Now for the answers: (1) The consequences of air ingress and wind washing for the hygrothermal performance and durability of well-insulated cathedral ceilings are very negative; there is worse thermal performance, problematic moisture response, and degraded durability. (2) A vented air space above the thermal insulation is not effective in humid, cool climates for preventing concealed condensation; it may even be negative in the sense that the venting paradigm weakens the attention for the really relevant performances and related good workmanship—avoiding exfiltration by applying an effective airflow barrier, minimizing wind washing by using an underlay with taped overlaps, and excluding air rotation around and in the insulation by applying a full fill between the airflow retarder and the underlay. (3) A vapor retarder is only efficient if airtightness is guaranteed. It works well on the condition that its vapor resistance accounts for the expected inside climate.

REFERENCES

ASHRAE. 1997. *1997 ASHRAE Handbook—Fundamentals*. Atlanta: American Society of Heating, Refrigerating and Air-Conditioning Engineers, Inc.

Bomberg, M., and J. Lstiburek. 1998. Field applied spray polyurethane foam in building envelopes. *Journal of Thermal Insulation and Building Envelopes*, Vol. 21, April, pp. 385-417.

Hens, H., B. Remans, E. Vanmechelen, and M. Hus. 1992. Pitched roofs: Heat-air-moisture transport in tiled and slated roofs with the thermal insulation at rafter level. Report 90/23, Laboratory of Building Physics, Department of Civil Engineering, University of Leuven, Belgium, 99 pp. (available on request).

Hens, H. 1994. Pitched roofs 2: HAM-transport in tiled and slated roofs with the thermal insulation at rafter level: Effects of air barrier and capillary underlay. Report 92/4, Laboratory of Building Physics, Department of Civil Engineering, University of Leuven, Belgium, 38 pp. (available on request).

Hens, H. 1992. Luft-Winddichtigkeit von geneigten Dächern: wie sie sich wirklich verhalten. *Bauphysik*, 14, Heft 6, pp. 161-174.

IEA. 1994a. *World energy outlook*. Paris: OECD/IEA, 305 pp.

IEA. 1994b. *A guidebook for insulated low-slope roof systems*. Annex 19, Low slope roof systems. Oak Ridge, Tenn.: Oak Ridge National Laboratory.

Janssens, A., and H. Hens. 1997. Water vapor transfer properties of spunbonded plastic films. *Journal of Thermal Insulation and Building Envelopes*, Vol. 21, Oct., pp. 202-220.

Janssens A., and H. Hens. 1995. VLIET proefgebouw (VLIET test building). Laboratory of Building Physics, Department of Civil Engineering, University of Leuven, Belgium, 43 pp.

Künzel, H. 1997. Steildächern, die Normvorschriften sind überholt. *Bundesbaublatt 46*, Heft 5, pp. 312-316.

Latta, J.K. 1974. Walls, windows and roofs for the Canadian climate. Special Technical Publication No. 1, National Research Council Canada.

LBP. 1981. Report 81/21, Laboratory of Building Physics, Department of Civil Engineering, University of Leuven, Belgium.

LBP. 1994. Report 94/1, Laboratory of Building Physics, Department of Civil Engineering, University of Leuven, Belgium.

Orr, H. 1974. Condensation in electrically heated houses. Paper 2.6.1. of the CIB/RILEM Symposium on Moisture Problems in Buildings, Rotterdam.

Redland Roof Tiles Ltd. 1988. *The Redland roofing manual 1989*. CTD Printers.

Rousseau, M. 1984. Control of surface and concealed condensation. *Building Science Insight 1983*, pp. 29-40. National Research Council Canada.